Model for the Viscoelastic and Viscoplastic Responses of Semicrystalline Polymers

Aleksey D. Drozdov, Jesper deClaville Christiansen

Department of Production, Aalborg University, Fibigerstraede 16, DK-9220 Aalborg, Denmark

Received 17 January 2002; accepted 14 May 2002

ABSTRACT: Constitutive equations are derived for the time-dependent behavior of semicrystalline polymers at isothermal loading with small strains. A semicrystalline polymer at temperatures above the glass-transition point for its amorphous phase is thought of as a network of macromolecules bridged by junctions (physical crosslinks, entanglements, and crystalline lamellae) that can slide with respect to their reference positions in the bulk material under straining. The network is assumed to be highly inhomogeneous, and it is modeled as an ensemble of mesoregions (MRs) with various strengths of interchain interaction. Two types of MRs are distinguished: passive, where these interactions prevent detachment of strands from junctions; and active, where active strands separate from junctions and dangling strands merge with the network at random times as they are thermally agitated. The viscoelastic response of a semicrystalline polymer reflects reformation of strands in active MRs, whereas its viscoplastic behavior is associated with sliding of junctions. Stress–strain relations for uniaxial deformation are developed by using the laws of thermodynamics. Adjustable parameters in the constitutive equations are found by fitting experimental data for isotactic polypropylene in a tensile test with a constant strain rate and in tensile relaxation tests at various strains. Fair agreement is demonstrated between the observations and the results of numerical simulation. It is revealed that the viscoplastic flow of junctions strongly affects the rearrangement process in active MRs, whose rate reaches a threshold value in the vicinity of the apparent yield point. © 2003 Wiley Periodicals, Inc. J Appl Polym Sci 88: 1438–1450, 2003

Key words: polypropylene; viscoelastic properties; relaxation; yielding; networks

INTRODUCTION

This study is concerned with modeling the time-dependent behavior of semicrystalline polymers at isothermal uniaxial deformation with small strains. Although the constitutive equations to be derived can be applied to the analysis of various semicrystalline polymers at room temperature (polyamides, polyethylene, polytetrafluorethylene, polypropylene, etc.), the work is concentrated on the response of isotactic polypropylene. The viscoelastic and viscoplastic behaviors of polypropylene have been a focus of attention in the past decade, which may be explained by numerous applications of this material in industry (oriented films for packaging, reinforcing fibers, nonwoven fabrics, polyethylene–polypropylene copolymers, blends of thermoplastic elastomers with polypropylene, etc.).

Despite a number of publications on the viscoplastic response of semicrystalline polymers, molecular mechanisms for yielding are still the subject of much debate. Roetling,[1–3] Peterlin and coauthors,[4–6] Flory and Yoon,[7] and Gent and Madan[8] attributed the yield behavior to mechanically induced melting and oriented recrystallization of lamellae under adiabatic conditions at temperatures far below the melting point. It is assumed that recrystallization of lamellae results in activation of molecular mobility in the amorphous phase, which is observed as an apparent yield at straining a specimen. A shortcoming of this approach is that melting of crystals is not thermally activated,[9] whereas the effects of temperature and strain rate on the yield stress are adequately predicted[10] by the Eyring equation for thermally activated processes.[11]

Another approach is based on conventional theories for crystal plasticity that treat yield of semicrystalline polymers as a process of nucleation, growth, and propagation of disclinations[12] and/or dislocations,[13] (see also Bordonaro and Krempl[14,15]). According to the dislocation–nucleation theory,[16–20] the yield point is associated with the beginning of nucleation of screw dislocations in crystalline lamellae whose Burgers' vectors are parallel to the chain axis. Propagation of these dislocations causes intralamellar slip. At small strains, this slip is homogeneous (fine slip recoverable after unloading at room temperature), whereas at large strains, it becomes heterogeneous (coarse slip) and induces fragmentation of lamellae into aligned blocks (see Figs. 16 to 18 in Coulon et al.[21]). An important advantage of this concept is that it provides a simple formula for the yield stress as a function of the

Correspondence to: A. D. Drozdov (drozdov@iprod.auc.dk).

Journal of Applied Polymer Science, Vol. 88, 1438–1450 (2003)

stem length, the magnitude of the Burgers vector, the Gibbs energy for nucleation of dislocations, and the shear modulus of crystallites.[22–24] A shortcoming of this theory is that it ignores the viscoelastic response of amorphous regions in a semicrystalline polymer, which implies that this approach is applicable either at relatively low temperatures (below the temperature of activation of the amorphous phase[18]) or at rather rapid loadings when the effect of viscocity is negligible.

According to the third approach, the time-dependent response of semicrystalline polymers is attributed to rearrangement of tie molecules that bridge lamellae.[25,26] Nitta and Takayanagi[27–29] associate yielding of a semicrystalline polymer with fragmentation of individual lamellae or lamellar clusters and model the postyield behavior as the process of pulling out of tie molecules (from fragmented lamellae), which merge with amorphous regions) (see Fig. 1 in Nitta and Takayanagi[29]).

A substantial disadvantage of these theories is that they do not establish a link between the viscoplastic and viscoelastic responses of semicrystalline polymers. The latter is conventionally treated in a purely phenomenological way either by using nonlinear stress–strain relations whose macroparameters do not reflect the microstructure of a polymer, or by constructing rheological (spring–dashpot) models without an adequate explanation of the physical meaning of individual elements.

The nonlinear viscoelastic response of polypropylene was studied by Ward and Wolfe[30] and Smart and Williams,[31] and, more recently, by Ariyama,[32–35] Wortmann and Schulz,[36,37] Dutta and Edward,[38] and Read and Tomlins.[39,40] In the past couple of years, the linear viscoelastic behavior of isotactic polypropylene was analyzed by Fricova et al.,[41] Andreassen,[42] Lopez-Manchado and Arroyo,[43] Gallego Ferrer et al.,[44] and Souza and Demarquette,[45] to mention a few. Two pronounced maxima were found on the graph of the loss tangent of isotactic polypropylene versus temperature: the first maximum (β-transition in the interval between $T = -20$ and $T = 10$°C) is associated with the glass transition in the most mobile part of the amorphous phase, whereas the other maximum (α-transition in the interval between $T = 50$ and $T = 80$°C) is attributed to the glass transition in the remaining part of the amorphous phase (the so-called rigid amorphous fraction[46]). This conclusion is confirmed by DSC (differential scanning calorimetry) traces for quenched polypropylene[9] that reveal an endoterm at $T = 70$°C, which can be ascribed to thermal activation of amorphous regions under heating.

Scanning electron microscopy and scanning force microscopy demonstrate that isotactic polypropylene is a semicrystalline polymer with a complicated morphology. The crystalline phase contains brittle monoclinic α-spherulites (the characteristic size of 100 μm) consisting of crystalline lamellae (10 to 20 nm in thickness) located in radial and tangential directions[21] and smectic mesophase. The structure of crystallites is not perfect and they contain a number of microdefects with various sizes. The amorphous phase is located inside the spherulites between lamellae and between spherulites. It consists of (i) relatively mobile chains between spherulites and between radial lamellae, and (ii) severely restricted chains in regions bounded by radial and tangential lamellae. Mechanical loading results in interlamellar separation, rotation and twist of lamellae, fine and coarse slip of lamellar blocks, and their fragmentation. The latter leads to reorganization of blocks and strain-induced smectic–monoclinic and monoclinic–smectic transitions.[9] Straining of a semicrystalline polymer causes chain slip through the crystals, breakage and reformation of tie chains, and activation of restricted amorphous regions driven by lamellar disintegration. In the postyield region, these transformations of microstructure lead to the onset of voids between lamellae, breakup of crystalls, and creation of fibrills.[47]

It is difficult to expect that these transformations of microstructure of polypropylene under loading may be captured in terms of a constitutive model with a relatively small number of adjustable parameters. To develop stress–strain relations for polypropylene, we apply the method of "homogenization of the microstructure into one phase whose internal micromechanical state is tracked as a function of applied deformation," recently proposed for the analysis of stresses in polyethylene.[48] As the phase under consideration, we choose the amorphous phase, which is explained by the following reasons:

1. The viscoelastic response of semicrystalline polymers is conventionally associated with rearrangement of chains in the amorphous regions.
2. The viscoplastic flow in semicrystalline polymers is supposed to be "initiated in the amorphous phase before transitioning into the crystalline phase."[49]
3. Sliding of tie chains along and their detachment from lamellae play the key role in the description of the yield phenomenon within the framework of the Takayanagi–Nitta concept.[27–29]
4. Conventional models for polyethylene,[48] polypropylene,[50,51] and poly(ethylene terephthalate)[52,53] disregard the crystalline phase and treat these polymers as equivalent networks of macromolecules.

Above the glass-transition temperature for the amorphous phase, a semicrystalline polymer is modeled as a network of macromolecules connected by junctions. Under loading, the junctions begin to slide with respect to their reference positions in the bulk material. Sliding of junctions models slippage of tie

molecules along lamellae, as well as fine slip of lamellar blocks. The viscoplastic response of a polymer is attributed to the sliding process. The network of polymeric chains is assumed to be strongly inhomogeneous, and it is treated as an ensemble of mesoregions (MRs) with various potential energies for detachment of chains from temporary nodes. Two types of MRs are distinguished: (i) active domains, where strands separate from junctions as they are thermally agitated (these MRs model a part of the amorphous phase that is free to be rearranged); and (ii) passive domains, where detachment of chains from junctions is prevented (these MRs are associated with the part of the amorphous phase whose mobility is restricted by radial and tangential lamellae). With reference to the theory of transient networks (see Green and Tobolsky,[54] Yamamoto,[55] Lodge,[56] and Tanaka and Edwards[57]), we assume that separation of active chains from their junctions and attachment of dangling chains to the network reflect the viscoelastic behavior of a semicrystalline polymer. Detachment of an active chain from a junction and merging of a dangling chain with the network occur at random times as the chains are thermally agitated.[57] In accord with the theory of thermally activated processes,[11] we suppose that the rate of detachment obeys the Eyring equation with a strain-dependent attempt rate. Deformation of a specimen results in (i) an increase in the concentration of active MRs (which is attributed to a partial release of the amorphous phase in passive mesodomains driven by fragmentation of lamellae) and (ii) a mechanically induced acceleration of separation of active chains from their junctions in active MRs.

The objective of this study is twofold:

1. to derive a constitutive model for the nonlinear viscoelastic and viscoplastic responses of semicrystalline polymers that can be implemented in finite element method (FEM) codes for numerical simulation.
2. to find adjustable parameters in the stress–strain relations by fitting experimental data in uniaxial tensile tests on isotactic polypropylene.

The exposition is organized as follows. The next section is concerned with kinetic equations for reformation of chains in active MRs and sliding of junctions. Afterward, we determine the strain energy density of a semicrystalline polymer and develop stress–strain relations for uniaxial deformation of a specimen by using the laws of thermodynamics. These constitutive equations are employed to fit experimental data in a tensile test with a constant strain rate and in tensile relaxation tests at several strains in the vicinity of the apparent yield point. The study is completed with some concluding remarks.

MICROMECHANICAL MODEL

A semicrystalline polymer is treated as a temporary network of chains bridged by junctions. The network is modeled as an ensemble of mesoregions (MRs) with various strengths of interaction between macromolecules. Two types of mesodomains are distinguished: passive and active. In passive MRs, interchain interactions prevent detachment of chains from junctions, which implies that all nodes in these domains are thought of as permanent. In active MRs, active strands (whose ends are connected to contiguous junctions) separate from the temporary junctions at random times when they are thermally agitated. An active chain whose end slips from a junction is transformed into a dangling chain. A dangling chain returns into the active state when its free end captures a nearby junction at a random instant.

Let X_a be the number of strands merged with the network in active MRs, and X_p the number of strands connected to the network in passive MRs. Under stretching some crystalline lamellae (restricting mobility of chains in passive MRs) break, which results in a growth of the number of strands that can be rearranged. As a consequence, the number of strands in active MRs increases and the number of strands in passive mesodomains decreases, which implies that the amounts X_a and X_p become functions of the current strain ε,

$$X_a = X_a(\varepsilon), \quad X_p = X_p(\varepsilon)$$

These quantities obey the conservation law

$$X_a(\varepsilon) + X_p(\varepsilon) = X \tag{1}$$

where X is the average number of active strands per unit mass of a polymer (which is assumed to be strain independent).

Detachment of active strands from temporary nodes in active MRs is thought of as a thermally activated process, whose rate is governed by the Eyring equation, whereas different mesodomains have different activation energies $\bar{\omega}$, for separation of strands from the network. According to the Eyring theory,[11] the rate of detachment of active strands in a MR with potential energy $\bar{\omega}$ in the stress-free state is given by

$$\Gamma = \Gamma_a \exp\left(-\frac{\bar{\omega}}{k_B T}\right)$$

where k_B is Boltzmann's constant, T is the absolute temperature, and the prefactor Γ_a is independent of energy $\bar{\omega}$ and temperature T. The attempt rate Γ_a may be associated with the rate of detachment of active strands at elevated temperatures ($T \to \infty$). Introducing the dimensionless potential energy

$$\omega = \frac{\bar{\omega}}{k_B T_0}$$

where T_0 is some reference temperature, and disregarding the effects of small increments of temperature, $\Delta T = T - T_0$, on the rate of separation Γ, we arrive at the formula

$$\Gamma = \Gamma_a \exp(-\omega) \tag{2}$$

In what follows, we suppose that eq. (2) is satisfied for an arbitrary loading process, provided that the attempt rate Γ_a is a function of strain $\Gamma_a = \Gamma_a(\varepsilon)$.

The distribution of active MRs with various potential energies is described by the probability density $p(\omega)$ that equals the ratio of the number $N_a(\varepsilon, \omega)$ of active mesodomains with energy ω to the total number of active MRs,

$$N_a(\varepsilon, \omega) = X_a(\varepsilon) p(\omega) \tag{3}$$

The distribution function for potential energies of active MRs $p(\omega)$ is assumed to be strain independent.

The ensemble of active mesodomains is entirely described by the function $n_a(t, \tau, \omega)$ that equals the number of active strands at time t (per unit mass) belonging to active MRs with potential energy ω that have last been rearranged before instant $\tau \in [0, t]$. In particular, $n_a(0, 0, \omega)$ is the number (per unit mass) of active strands in active MRs with potential energy ω in a stress-free medium,

$$n_a(0, 0, \omega) = N_a(0, \omega) \tag{4}$$

and $n_a(t, t, \omega)$ is the number (per unit mass) of active strands in active MRs with potential energy ω in the deformed medium at time t (the initial time $t = 0$ corresponds to the instant when external loads are applied to a specimen),

$$n_a(t, t, \omega) = N_a(\varepsilon(t), \omega) \tag{5}$$

The amount

$$\frac{\partial n_a}{\partial \tau}(t, \tau, \omega)\Big|_{t=\tau} d\tau$$

equals the number (per unit mass) of dangling strands in active MRs with potential energy ω that merge with the network within the interval $[\tau, \tau + d\tau]$, and the quantity

$$\frac{\partial n_a}{\partial \tau}(t, \tau, \omega)\, d\tau$$

is the number of these strands that have not detached from temporary junctions during the interval $[\tau, t]$. The number (per unit mass) of strands in active MRs that separate (for the first time) from the network within the interval $[t, t + dt]$ reads

$$-\frac{\partial n_a}{\partial t}(t, 0, \omega)\, dt$$

whereas the number (per unit mass) of strands in active MRs that merged with the network during the interval $[\tau, \tau + d\tau]$ and, afterward, separate from the network within the interval $[t, t + dt]$ is given by

$$-\frac{\partial^2 n_a}{\partial t\, \partial \tau}(t, \tau, \omega)\, dt\, d\tau$$

The rate of separation Γ equals the ratio of the number of active strands that detach from the network per unit time to the current number of active strands. Applying this definition to active strands that merged with the network during the interval $[\tau, \tau + d\tau]$ and separate from temporary junctions within the interval $[t, t + dt]$, we find that

$$\frac{\partial^2 n_a}{\partial t\, \partial \tau}(t, \tau, \omega) = -\Gamma(\varepsilon(t), \omega) \frac{\partial n_a}{\partial \tau}(t, \tau, \omega) \tag{6}$$

To describe changes in the function $n_a(t, 0, \omega)$, two processes should be taken into account: (i) detachment of active strands from temporary nodes, and (ii) transition of passive mesodomains into the active state under loading. The kinetic equation for this function reads

$$\frac{\partial n_a}{\partial t}(t, 0, \omega) = -\Gamma(\varepsilon(t), \omega) n_a(t, 0, \omega) + \frac{\partial N_a}{\partial \varepsilon}(\varepsilon(t), \omega) \frac{d\varepsilon}{dt}(t) \tag{7}$$

The solution of eq. (7) with initial condition (4) is given by

$$n_a(t, 0, \omega) = N_a(0, \omega) \exp\left[-\int_0^t \Gamma(\varepsilon(s), \omega)\, ds\right] + \int_0^t \frac{\partial N_a}{\partial \varepsilon}(\varepsilon(\tau), \omega) \frac{d\varepsilon}{dt}(\tau) \exp\left[-\int_\tau^t \Gamma(\varepsilon(s), \omega)\, ds\right] d\tau \tag{8}$$

It follows from eq. (6) that

$$\frac{\partial n_a}{\partial \tau}(t, \tau, \omega) = \varphi(\tau, \omega)\exp\left[-\int_\tau^t \Gamma(\varepsilon(s), \omega)\, ds\right] \quad (9)$$

where

$$\varphi(\tau, \omega) = \frac{\partial n_a}{\partial \tau}(t, \tau, \omega)\Big|_{t=\tau} \quad (10)$$

To determine the function $\varphi(t, \omega)$, we use the identity

$$n_a(t, t, \omega) = n_a(t, 0, \omega) + \int_0^t \frac{\partial n_a}{\partial \tau}(t, \tau, \omega)\, d\tau \quad (11)$$

Equations (5) and (11) imply that

$$n_a(t, 0, \omega) + \int_0^t \frac{\partial n_a}{\partial \tau}(t, \tau, \omega)\, d\tau = N_a(\varepsilon(t), \omega) \quad (12)$$

Differentiating eq. (12) with respect to time and using eq. (10), we obtain

$$\varphi(t, \omega) + \frac{\partial n_a}{\partial t}(t, 0, \omega) + \int_0^t \frac{\partial^2 n_a}{\partial t\, \partial \tau}(t, \tau, \omega)\, d\tau = \frac{\partial N_a}{\partial \varepsilon}(\varepsilon(t), \omega)\frac{d\varepsilon}{dt}(t)$$

This equality together with eqs. (6), (7), and (11) results in

$$\varphi(t, \omega) = \Gamma(\varepsilon(t), \omega)\left[n_a(t, 0, \omega) + \int_0^t \frac{\partial n_a}{\partial \tau}(t, \tau, \omega)\, d\tau\right] = \Gamma(\varepsilon(t), \omega) n_a(t, t, \omega) \quad (13)$$

Substituting expression (13) into eq. (9) and using eq. (5), we arrive at the formula

$$\frac{\partial n_a}{\partial \tau}(t, \tau, \omega) = \Gamma(\varepsilon(t), \omega) N_a(\varepsilon(t), \omega)\exp\left[-\int_\tau^t \Gamma(\varepsilon(s), \omega)\, ds\right] \quad (14)$$

Changes in the function $n_a(t, \tau, \omega)$, and, as a consequence, the kinetics of rearrangement of strands in active MRs are described by eqs. (2), (3), (8), and (14). These relations are determined by (i) the distribution function $p(\omega)$ for active MRs with various potential energies ω, (ii) the function $\Gamma_a(\varepsilon)$ that characterizes the effect of strains on the attempt rate, and (iii) the function

$$\kappa_a(\varepsilon) = \frac{X_a(\varepsilon)}{X} \quad (15)$$

that reflects mechanically induced activation of passive MRs.

Separation of active strands from their junctions and merging of dangling chains with the temporary network in active MRs reflect the viscoelastic response of a semicrystalline polymer. The viscoplastic behavior is associated with strain-induced slippage of junctions with respect to their positions in the bulk material.

Denote by $\varepsilon_u(t)$ the average strain induced by sliding of junctions between macromolecules (the subscript index "u" means that $\varepsilon_u(t)$ is associated with the residual strain in a specimen which is suddenly unloaded at instant t). Let $\varepsilon_e(t)$ be the elastic strain (which reflects elongation of active strands in a network). The functions $\varepsilon_e(t)$ and $\varepsilon_u(t)$ are connected with the macrostrain $\varepsilon(t)$ by the conventional formula

$$\varepsilon(t) = \varepsilon_e(t) + \varepsilon_u(t) \quad (16)$$

We adopt the first-order kinetics for sliding of junctions, which implies that the increment of the viscoplastic strain $d\varepsilon_u$, induced by the growth of the macrostrain ε by an increment $d\varepsilon$, is proportional to the absolute value of the stress σ,

$$\frac{d\varepsilon_u}{d\varepsilon} = B|\sigma|\,\mathrm{sign}\left(\sigma\frac{d\varepsilon}{dt}\right) \quad (17)$$

where the prefactor B is a function of the macrostrain ε and the sign function is given by

$$\mathrm{sign}(x) = \begin{cases} -1, & x < 0 \\ 0, & x = 0 \\ 1, & x > 0 \end{cases}$$

The last multiplier in eq. (17) determines the direction of the viscoplastic flow of junctions.

To explain the dependency of the coefficient B of strain, we suppose that not all junctions in a stress-free specimen are involved into the sliding process. Denote by $Y(\varepsilon)$ the number of strands (per unit mass) whose ends are linked to sliding junctions when the macrostrain in a sample equals ε. To describe release of the amorphous phase in passive mesodomains driven by fragmentation of lamellae, we suppose that for a virgin specimen, the function $Y(\varepsilon)$ monotonically increases with the absolute value of macrostrain $|\varepsilon|$ from some initial value $Y(0)$ that characterizes the concentration of mobile junctions in a stress-free medium, to a final value

$$Y(\varepsilon_0) = X \tag{18}$$

which is reached at some threshold strain ε_0. The function $Y(\varepsilon)$ is given by

$$Y(\varepsilon) = \eta(\varepsilon)X$$

where $\eta(\varepsilon)$ is the concentration of active strands whose ends are bridged to mobile junctions. The average rate of sliding B is assumed to be proportional to the concentration of junctions involved in the sliding process,

$$B = b\eta$$

where b is the rate of sliding in a network where all junctions slide with respect to their reference positions. Substitution of this equality into eq. (17) implies the differential equation

$$\frac{d\varepsilon_u}{dt}(t) = b\eta(\varepsilon(t))|\sigma(t)|\mathrm{sign}\left[\sigma(t)\frac{d\varepsilon}{dt}(t)\right]\frac{d\varepsilon}{dt}(t), \qquad \varepsilon_u(0) = 0 \tag{19}$$

According to eq. (19), the kinetics of sliding of junctions is entirely determined by (i) the rate of sliding b in a network with all mobile nodes and (ii) the current concentration of mobile junctions $\eta(\varepsilon)$.

To describe mechanically induced transformation of immobile junctions into mobile ones, we treat this transition as a self-accelerating (avalanch-like) process. This means that the growth of the macrostrain ε by an increment $d\varepsilon$ implies an increase in the function $\eta(\varepsilon)$ by an increment $d\eta$, which is proportional to the concentration of mobile junctions in the vicinity of those to be included into the sliding process,

$$\frac{d\eta}{d\varepsilon}(\varepsilon) = a\eta(\varepsilon)\mathrm{sign}\left(\sigma\frac{d\varepsilon}{dt}\right), \quad |\varepsilon| \le \varepsilon_0$$

$$\frac{d\eta}{d\varepsilon}(\varepsilon) = 0, \quad |\varepsilon| > \varepsilon_0 \tag{20}$$

where the rate of transformation a is found by matching observations (in general, a is a function of the strain rate) and the constant ε_0 is determined by condition (18).

For active straining with a constant strain rate $d\varepsilon(t)/dt > 0$, the solution of differential eq. (20) with boundary condition (18) reads

$$\eta(\varepsilon) = \begin{cases} \exp[a(\varepsilon - \varepsilon_0)], & 0 \le \varepsilon < \varepsilon_0 \\ 1, & \varepsilon_0 \le \varepsilon < \infty \end{cases}$$

CONSTITUTIVE EQUATIONS

Any strand is modeled as a linear elastic solid with the mechanical energy

$$w = \tfrac{1}{2}\mu e^2 \tag{21}$$

where μ is the average rigidity per strand and e is the strain from the stress-free state to the deformed state of the strand.

For strands belonging to passive mesodomains, the strain $e(t)$ coincides with $\varepsilon_e(t)$. Multiplying the strain energy per strand by the number of strands in passive MRs, we find the mechanical energy of mesodomains where rearrangement of chains is prevented by surrounding macromolecules,

$$W_p(t) = \tfrac{1}{2}\mu X_p(\varepsilon(t))\varepsilon_e^2(t) \tag{22}$$

With reference to the conventional theory of temporary networks,[57] we assume that stresses in dangling strands totally relax before they merge with the network. This implies that the reference (stress-free) state of a strand that merges with the network at time $\tau \in [0, t]$ coincides with the deformed state of the network at that instant. For active strands that have not been rearranged until time t, the strain $e(t)$ coincides with $\varepsilon_e(t)$, whereas for active strands that have last been merged with the network at time $\tau \in [0, t]$, the strain $e(t, \tau)$ is given by

$$e(t, \tau) = \varepsilon_e(t) - \varepsilon_e(\tau)$$

Summing the mechanical energies of active strands belonging to active MRs with various activation energies ω, that were rearranged at various instants τ, we find the mechanical energy of active mesodomains,

$$W_a(t) = \frac{1}{2}\mu\int_0^\infty d\omega\left\{n_a(t, 0, \omega)\varepsilon_e^2(t) + \int_0^t \frac{\partial n_a}{\partial\tau}(t, \tau, \omega) \times [\varepsilon_e(t) - \varepsilon_e(\tau)]^2\, d\tau\right\} \tag{23}$$

The mechanical energy per unit mass of a polymer reads

$$W(t) = W_a(t) + W_p(t)$$

Substituting expressions (22) and (23) into this equality and using eq. (16), we arrive at the formula

$$W(t) = \frac{1}{2}\,\mu\Bigg\{ X_p(\varepsilon(t))(\varepsilon(t) - \varepsilon_u(t))^2 + \int_0^\infty d\omega\Bigg[n_a(t, 0, \omega)(\varepsilon(t) - \varepsilon_u(t))^2 + \int_0^t \frac{\partial n_a}{\partial \tau}(t, \tau, \omega) \times ((\varepsilon(t) - \varepsilon_u(t)) - (\varepsilon(\tau) - \varepsilon_u(\tau)))^2\, d\tau\Bigg]\Bigg\} \quad (24)$$

Differentiation of eq. (24) with respect to time results in

$$\frac{dW}{dt}(t) = \mu A(t)\left[\frac{d\varepsilon}{dt}(t) - \frac{d\varepsilon_u}{dt}(t)\right] + \frac{1}{2}\,\mu A_0(t) \quad (25)$$

where

$$A(t) = X_p(\varepsilon(t))[\varepsilon(t) - \varepsilon_u(t)] + \int_0^\infty d\omega\Bigg\{ n_a(t, 0, \omega) \times [\varepsilon(t) - \varepsilon_u(t)] + \int_0^t \frac{\partial n_a}{\partial \tau}(t, \tau, \omega)[(\varepsilon(t) - \varepsilon_u(t)) - (\varepsilon(\tau) - \varepsilon_u(\tau))]\, d\tau\Bigg\}$$

$$A_0(t) = \frac{\partial X_p}{\partial \varepsilon}(\varepsilon(t))\frac{d\varepsilon}{dt}(t)[\varepsilon(t) - \varepsilon_u(t)]^2 + \int_0^\infty d\omega\Bigg\{ \frac{\partial n_a}{\partial t}(t, 0, \omega)[\varepsilon(t) - \varepsilon_u(t)]^2 + \int_0^t \frac{\partial^2 n_a}{\partial t\,\partial \tau}(t, \tau, \omega)[(\varepsilon(t) - \varepsilon_u(t)) - (\varepsilon(\tau) - \varepsilon_u(\tau))]^2\, d\tau\Bigg\} \quad (26)$$

Bearing in mind eqs. (5) and (11), we transform the first equality in eq. (26) as follows:

$$A(t) = [X_p(\varepsilon(t)) + \int_0^\infty N_a(\varepsilon(t), \omega)\, d\omega][\varepsilon(t) - \varepsilon_u(t)] - \int_0^\infty d\omega \int_0^t \frac{\partial n_a}{\partial \tau}(t, \tau, \omega)[\varepsilon(\tau) - \varepsilon_u(\tau)]\, d\tau$$

This formula together with eqs. (1) and (3) implies that

$$A(t) = X[\varepsilon(t) - \varepsilon_u(t)] - \int_0^\infty d\omega \int_0^t \frac{\partial n_a}{\partial \tau}(t, \tau, \omega)[\varepsilon(\tau) - \varepsilon_u(\tau)]\, d\tau \quad (27)$$

Substitution of expressions (6) and (7) into the second equality in eq. (26) yields

$$A_0(t) = \left[\frac{\partial X_p}{\partial \varepsilon}(\varepsilon(t)) + \int_0^\infty \frac{\partial N_a}{\partial \varepsilon}(\varepsilon(t), \omega)\, d\omega\right]\frac{d\varepsilon}{dt}(t) \times [\varepsilon(t) - \varepsilon_u(t)]^2 - A_1(t) \quad (28)$$

where

$$A_1(t) = \int_0^\infty \Gamma(\varepsilon(t), \omega)\, d\omega\Bigg\{ n_a(t, 0, \omega)[\varepsilon(t) - \varepsilon_u(t)]^2 + \int_0^t \frac{\partial n_a}{\partial \tau}(t, \tau, \omega)[(\varepsilon(t) - \varepsilon_u(t)) - (\varepsilon(\tau) - \varepsilon_u(\tau))]^2\, d\tau\Bigg\} \quad (29)$$

It follows from eqs. (1), (3), and (28) that

$$A_0(t) = -A_1(t)$$

This equality together with eq. (25) results in

$$\frac{dW}{dt}(t) = \mu\left[A(t)\frac{d\varepsilon}{dt}(t) - \frac{1}{2}(A_1(t) + A_2(t))\right] \quad (30)$$

where

$$A_2(t) = 2A(t)\frac{d\varepsilon_u}{dt}(t) \quad (31)$$

For uniaxial loading with small strains at the reference temperature T_0, the Clausius–Duhem inequality reads

$$T_0\frac{dQ}{dt}(t) = -\frac{dW}{dt}(t) + \frac{1}{\rho}\sigma(t)\frac{d\varepsilon}{dt}(t) \geq 0 \quad (32)$$

where ρ is mass density and Q is the entropy production per unit mass. Substitution of expression (30) into eq. (32) implies that

$$T_0\frac{dQ}{dt}(t) = \frac{1}{\rho}[\sigma(t) - \rho\mu A(t)]\frac{d\varepsilon}{dt}(t) + \frac{1}{2}[A_1(t) + A_2(t)] \geq 0 \quad (33)$$

Because eq. (33) is to be fulfilled for an arbitrary program of straining $\varepsilon = \varepsilon(t)$, the expression in the first square brackets vanishes. This assertion together with eq. (27) results in the stress–strain relation

$$\sigma(t) = \rho\mu A(t) = E\left\{[\varepsilon(t) - \varepsilon_u(t)] - \frac{1}{X}\int_0^\infty d\omega \int_0^t \frac{\partial n_a}{\partial \tau}(t, \tau, \omega) \times [\varepsilon(\tau) - \varepsilon_u(\tau)]\, d\tau\right\} \quad (34)$$

where

$$E = \rho\mu X$$

is an analog of Young's modulus. It follows from eqs. (19), (31), and (34) that

$$A_2(t) = \frac{2b}{\rho\mu}\,\eta(\varepsilon(t))\sigma^2(t)\left|\frac{d\varepsilon}{dt}(t)\right| \quad (35)$$

According to eqs. (29) and (35), the functions $A_1(t)$ and $A_2(t)$ are nonnegative, which, together with eq. (34), implies that the Clausius–Duhem inequality (33) is satisfied.

Substitution of eqs. (3), (14), and (15) into eq. (34) results in the constitutive equation

$$\sigma(t) = E\left\{[\varepsilon(t) - \varepsilon_u(t)] - \kappa_a(\varepsilon(t))\int_0^\infty p(\omega)\, d\omega \times \int_0^t \Gamma(\varepsilon(t), \omega)\exp\left[-\int_\tau^t \Gamma(\varepsilon(s), \omega)\, ds\right][\varepsilon(\tau) - \varepsilon_u(\tau)]\, d\tau\right\} \quad (36)$$

Given functions $p(\omega)$, $\Gamma_a(\varepsilon)$, and $\kappa_a(\varepsilon)$, eqs. (2), (19), (20), and (36) describe the time-dependent response of a semicrystalline polymer at isothermal uniaxial loading with small strains.

For rapid loadings, when the influence of rearrangement of active strands on the mechanical response is negligible, eq. (36) reads

$$\sigma = E(\varepsilon - \varepsilon_u) \quad (37)$$

Equations (19), (20), and (37) are determined by four adjustable parameters:

1. the elastic modulus E
2. the rate of activation of immobile junctions a
3. the rate of sliding of junctions b
4. the threshold strain ε_0

This number is quite comparable with the number of material constants used in other models for the viscoplastic response of semicrystalline polymers (see, e.g., Refs. 14, 15, 23, 24, 27, 58–60).

For a standard relaxation test with the longitudinal strain ε^0,

$$\varepsilon(t) = \begin{cases} 0, & t < 0 \\ \varepsilon^0, & t \geq 0 \end{cases}$$

equations (2), (19), (20), and (36) imply that

$$\sigma(t, \varepsilon^0) = E(\varepsilon^0 - \varepsilon_u^0)\{1 - \kappa_a(\varepsilon^0)\int_0^\infty p(\omega)[1 - \exp(-\Gamma_a(\varepsilon^0)\exp(-\omega)t)]\, d\omega\} \quad (38)$$

where ε_u^0 is the strain induced by sliding of junctions. Introducing the dimensionless ratio of the current stress at time t to the initial stress at the instant $t = 0$,

$$R(t, \varepsilon^0) = \frac{\sigma(t, \varepsilon^0)}{\sigma(0, \varepsilon^0)} \quad (39)$$

we find from eq. (38) that

$$R(t, \varepsilon^0) = 1 - \kappa_a(\varepsilon^0)\int_0^\infty p(\omega)[1 - \exp(-\Gamma_a(\varepsilon^0)\exp(-\omega)t)]\, d\omega \quad (40)$$

To fit experimental data, we adopt the random energy model[61] with

$$p(\omega) = p_0\exp\left[-\frac{(\omega - \Omega)^2}{2\Sigma^2}\right], \quad \omega \geq 0, \quad p(\omega) = 0, \quad \omega < 0 \quad (41)$$

where Ω and Σ are adjustable parameters, and the prefactor p_0 is determined by the condition

$$\int_0^\infty p(\omega)\, d\omega = 1 \quad (42)$$

Given a strain ε^0, eqs. (40) and (41) are determined by four material constants:

1. the average potential energy for rearrangement of strands Ω
2. the standard deviation of potential energies Σ
3. the attempt rate for separation of strands in active MRs Γ_a

4. the concentration of strands in active mesodomains κ_a

These parameters are found by matching experimental data for isotactic polypropylene.

EXPERIMENTAL

A series of uniaxial tests on polypropylene specimens was performed at room temperature. Isotactic polypropylene (Novolen 1100L) was supplied by BASF (Targor). ASTM dumbbell-shape specimens with length 148 mm, width 10 mm, and thickness 3.8 mm were injection molded and used without any thermal pretreatment. Our DSC measurements (the sample mass 16.4 mg, the heating rate 10 K/min) demonstrated the specific enthalpy of melting $\Delta H_m = 77.6$ J/g. This value of ΔH_m is quite comparable with the enthalpy of melting 78.1 J/g found by Collar et al.,[62] and corresponds to the degree of crystallinity $\kappa_c = 0.37$ (when the value 209 J/g[63] is accepted as the enthalpy of fusion for a fully crystalline polypropylene).

Mechanical experiments were carried out with the use of a testing machine Instron 5568 equipped with sensors for the control of longitudinal strains in the active zone of samples (with the distance between clips 50 mm). The tensile force was measured by a standard load cell. The engineering stress σ was determined as the ratio of the axial force to the cross-sectional area of the specimens in the stress-free state (38 mm^2).

A uniaxial tensile test was performed with the constant cross-head speed 2 mm/min (which corresponds

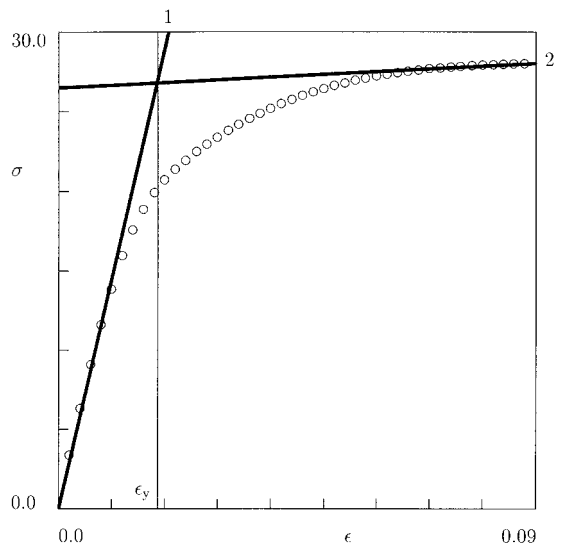

Figure 1 Stress σ (MPa) versus strain ε in a tensile test with strain rate $\dot{\varepsilon}_0 = 0.02$ min^{-1}. Circles: experimental data. Solid lines 1 and 2 denote tangent directions at small and large strains.

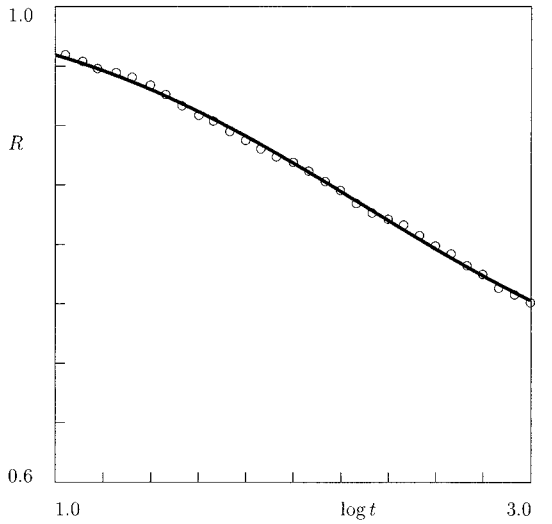

Figure 2 Dimensionless ratio R versus time t(s) in a tensile relaxation test with strain $\varepsilon_1 = 0.0086$. Circles: experimental data. Solid line: results of numerical simulation.

to the strain rate $\dot{\varepsilon}_0 = 0.02$ min^{-1}) up to the maximal strain $\varepsilon_{max} = 0.09$. The stress–strain diagram is depicted in Figure 1. To assess the apparent yield point, we employ the following approach[10]: the apparent yield strain ε_y is determined as the point of intersection of two tangent lines to the stress–strain curve. The first straight line corresponds to small strains, and its slope characterizes the initial Young's modulus (curve 1 in Fig. 1), whereas the other line is determined at relatively large strains (curve 2 in Fig. 1). The intersection point for these two lines results in the value $\varepsilon_y = 0.019$. It is worth noting that this method provides a rather rough estimate of the apparent yield point (it strongly depends on which strains are assumed to be "large" to draw the tangent straight-line 2 in Fig. 1). We accept this estimate, however, to compare the apparent yield strain with other critical parameters of the model.

A series of relaxation tests was carried out at the strains $\varepsilon_1 = 0.0086$ (this strain corresponds to the transition from the linear viscoelastic regime to the nonlinear viscoelastic regime of deformation; see Fig. 1), $\varepsilon_2 = 0.02$ (this strain is associated with the apparent yield strain ε_y on the stress–strain diagram), and three strains: $\varepsilon_3 = 0.03$, $\varepsilon_4 = 0.04$, and $\varepsilon_5 = 0.06$ exceeding the strain ε_y. In these tests, specimens were loaded with the strain rate $\dot{\varepsilon}_0$ up to a given strain level that was preserved constant during the relaxation time ($t_r = 20$ min).

In any relaxation test, the dimensionless ratio of stresses R was determined as a function of time t (the initial instant $t = 0$ corresponds to the beginning of the relaxation process) and was plotted versus the logarithm of time (log = $\log_{10}$) in Figures 2 to 6. These figures demonstrate that the amount of relaxing stress

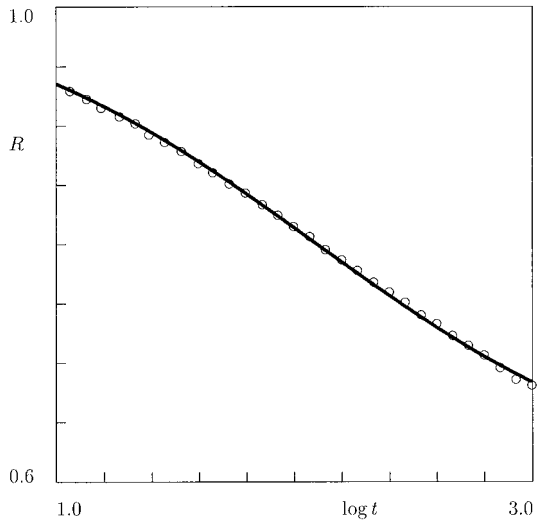

Figure 3 Dimensionless ratio R versus time t(s) in a tensile relaxation test with strain $\varepsilon_2 = 0.02$. Circles: experimental data. Solid line: results of numerical simulation.

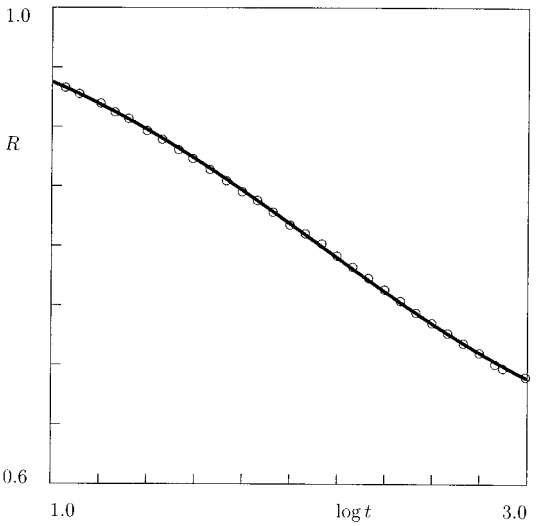

Figure 5 Dimensionless ratio R versus time t(s) in a tensile relaxation test with strain $\varepsilon_4 = 0.04$. Circles: experimental data. Solid line: results of numerical simulation.

increases with strain ε in the interval $[0, \varepsilon_y]$ and remains practically constant at strains exceeding ε_y.

FITTING OF EXPERIMENTAL DATA

We begin with matching observations in a tensile test with the constant strain rate $\dot{\varepsilon}_0$. For this purpose, we fix the intervals $[0, a_{\max}]$, $[0, c_{\max}]$, and $[0, h_{\max}]$, where the best-fit parameters a, $c = Eb$, and $h = \eta(0)$ are assumed to be found and divide these intervals into J subintervals by the points $a_i = i\Delta_a$, $b_j = j\Delta_b$, and $h_k = k\Delta_h$ $(i, j, k = 1, \ldots, J)$, with $\Delta_a = a_{\max}/J$, $\Delta_b = b_{\max}/J$, and $\Delta_h = h_{\max}/J$. For any triple $\{a_i, c_j, h_k\}$, we integrate numerically governing eqs. (19), (20), and (37),

$$\frac{d\varepsilon_u}{d\varepsilon} = c_j\eta(\varepsilon - \varepsilon_u), \quad \varepsilon_u(0) = 0,$$

$$\frac{d\eta}{d\varepsilon} = a_i\eta H(1 - \eta), \quad \eta(0) = h_k$$

in the interval $[0, \varepsilon_{\max}]$ by the Runge–Kutta method with the step $\Delta_\varepsilon = 10^{-4}$. Here we use the notation

$$H(x) = \begin{cases} 1, & x \geq 0 \\ 0, & x < 0 \end{cases}$$

The Young's modulus $E = E(i, j, k)$ (which ensures the best approximation of the experimental stress–strain

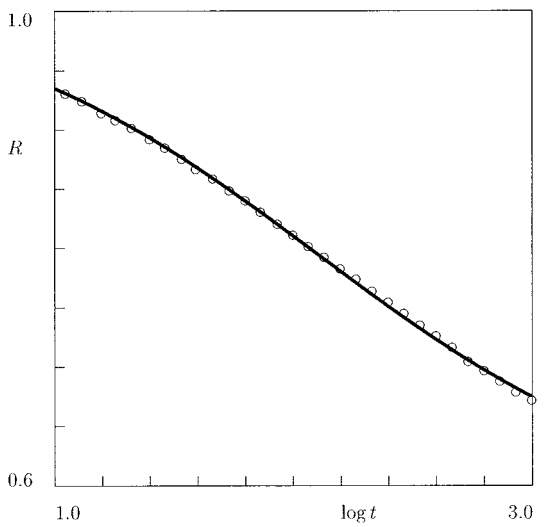

Figure 4 Dimensionless ratio R versus time t(s) in a tensile relaxation test with strain $\varepsilon_3 = 0.03$. Circles: experimental data. Solid line: results of numerical simulation.

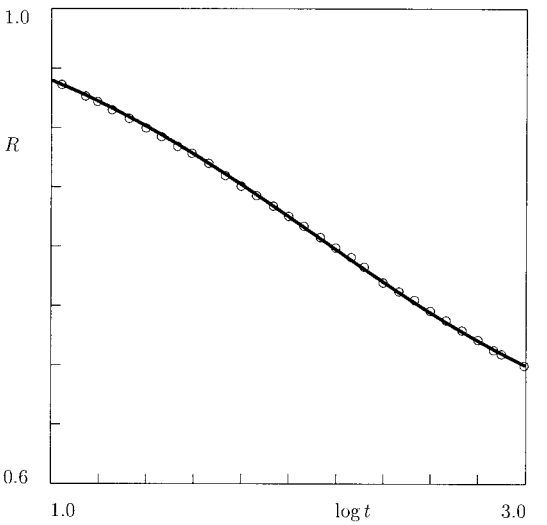

Figure 6 Dimensionless ratio R versus time t(s) in a tensile relaxation test with strain $\varepsilon_5 = 0.06$. Circles: experimental data. Solid line: results of numerical simulation.

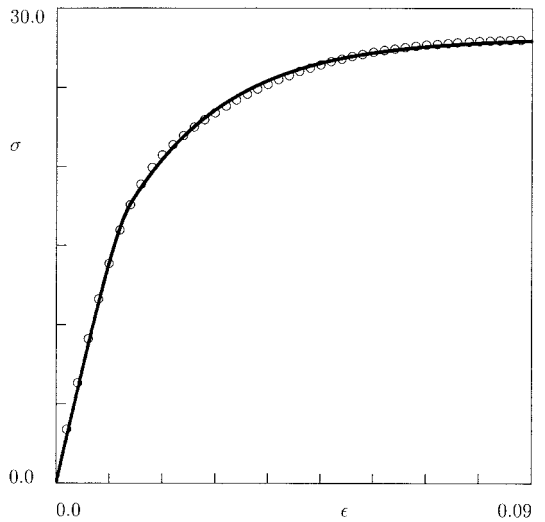

Figure 7 Stress σ (MPa) versus strain ε in a tensile test with strain rate $\dot{\varepsilon}_0 = 0.02$ min^{-1}. Circles: experimental data. Solid line: results of numerical simulation with $E = 1.46$ GPa, $a = 230.0$, $b = 0.036$ MPa^{-1}, and $\eta(0) = 0.04$.

diagram) is determined by the least-squares method. As a measure of discrepancy between observations and results of numerical analysis, we choose the function

$$F(i, j, k) = \sum_{\varepsilon_m} [\sigma_{\exp}(\varepsilon_m) - \sigma_{\text{num}}(\varepsilon_m)]^2$$

where the sum is calculated over all experimental points ε_m, depicted in Figure 1, and the function $\sigma_{\text{num}}(\varepsilon_m)$ is given by eq. (37). The optimal parameters a, c, and h minimize the function F on the set

$$\{a_i, c_j, h_k \quad (i, j, k = 1, \ldots, J)\}$$

To ensure good accuracy of fitting, after finding the best-fit parameters a_i, c_j, and h_k, this procedure is repeated for the new intervals $[a_{i-1}, a_{i+1}]$, $[c_{j-1}, c_{j+1}]$, and $[h_{k-1}, h_{k+1}]$. The threshold strain $\varepsilon_0 = 0.014$ is determined from the condition $\eta(\varepsilon_0) = 0.9995$.

Figure 7 demonstrates fair agreement between the experimental data and the results of numerical simulation. The value of Young's modulus $E = 1.46$ GPa, found by fitting observations, is rather close to the value $E = 1.50$ GPa provided by the supplier. The apparent yield strain $\varepsilon_y = 0.019$ slightly exceeds the strain ε_0 at which all junctions become mobile. It is worth noting a rather low value of the concentration of mobile junctions in a stress-free polymer $\eta(0) = 0.04$, which indicates that most junctions are activated under straining.

To match observations in relaxation tests, we begin with the relaxation curve at the minimum strain, $\varepsilon_1 = 0.0086$. Because the attempt rate Γ_a and the average potential energy Ω are mutually dependent [eq. (40) implies that the growth of Ω results in an increase in Γ_a], we set $\Gamma_a = 1$ s and approximate the relaxation curve at ε_1 by using three experimental constants: Ω, Σ, and κ_a. To find these parameters, we employ a procedure similar to that used in fitting the stress–strain curve. We fix the intervals $[0, \Omega_{\max}]$ and $[0, \Sigma_{\max}]$, where the best-fit parameters Ω and Σ are assumed to be located, and divide these intervals into J subintervals by the points $\Omega_i = i\Delta_\Omega$ and $\Sigma_j = j\Delta_\Sigma$ ($i, j = 1, \ldots, J$) with $\Delta_\Omega = \Omega_{\max}/J$, $\Delta_\Sigma = \Sigma_{\max}/J$. For any pair $\{\Omega_i, \Sigma_j\}$, we evaluate the integral in eq. (40) numerically (by Simpson's method with 200 points and the step $\Delta_\omega = 0.1$). The prefactor p_0 is determined by eq. (41). The parameter $\kappa_a = \kappa_a(i, j)$ is found by the least-squares technique from the condition of minimum of the function

$$F(i, j) = \sum_{t_m} [R_{\exp}(t_m) - R_{\text{num}}(t_m)]^2$$

where the sum is calculated over all experimental points t_m, depicted in Figure 2, and the function $R_{\text{num}}(t_m)$ is given by eq. (41). The optimal parameters Ω and Σ minimize the function F on the set

$$\{\Omega_i, \Sigma_j \ (i, j = 1, \ldots, J)\}$$

After finding the best-fit parameters Ω_i and Σ_j, this procedure is repeated twice for the new intervals $[\Omega_{i-1}, \Omega_{i+1}]$ and $[\Sigma_{j-1}, \Sigma_{j+1}]$ to ensure good accuracy of fitting. Figure 2 shows excellent agreement between the experimental data and the results of numerical simulation with $\Omega = 5.71$ and $\Sigma = 2.14$.

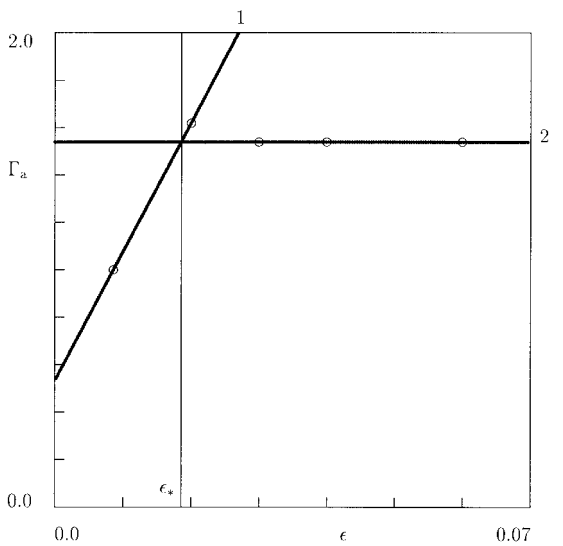

Figure 8 Attempt rate Γ_a(s^{-1}) versus strain ε. Circles: treatment of observations in tensile relaxation tests. Solid lines: approximation of experimental data by eq. (43). Curve 1: $\Gamma_{a0} = 0.53$, $\Gamma_{a1} = 54.39$; curve 2: $\Gamma_a^\circ = 1.54$.

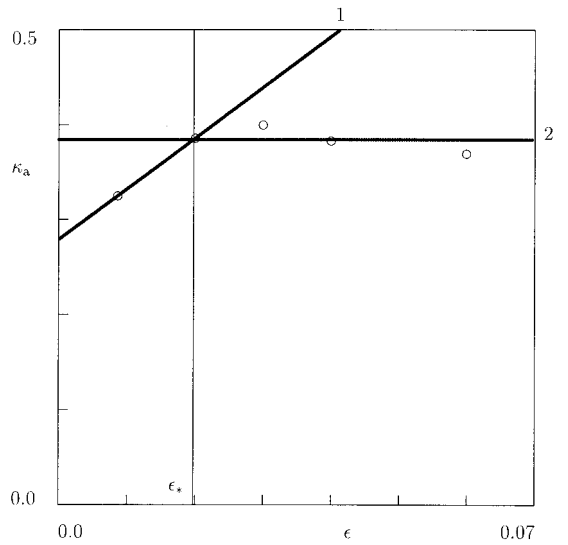

Figure 9. Fraction of active MRs κ_a versus strain ε. Circles: treatment of observations in tensile relaxation tests. Solid lines: approximation of experimental data by eq. (43). Curve 1: $\kappa_{a0} = 0.28$, $\kappa_{a1} = 5.35$; curve 2: $\kappa_a^\circ = 0.38$.

To approximate observations in relaxation tests at higher strains, we fix the constants Ω and Σ found by matching experimental data at ε_1 and fit every relaxation curve by using two adjustable parameters: Γ_a and κ_a. Given a value of κ_a, the attempt rate Γ_a is determined by the steepest descent algorithm. The concentration of active MRs κ_a is found by the least-squares method. Figures 3 to 6 demonstrate fair agreement between the observations and the results of numerical analysis.

The parameters Γ_a and κ_a are plotted versus the longitudinal strain ε in Figures 8 and 9. The quantities Γ_a and κ_a linearly increase with strain ε in the region of nonlinear viscoelasticity and reach their maximum values at the strain $\varepsilon_* \approx 0.019$, which coincides with the apparent yield strain ε_y. At $\varepsilon \geq \varepsilon_*$, the attempt rate Γ_a and the concentration of active MRs κ_a remain constant,

$$\Gamma_a = \Gamma_{a0} + \Gamma_{a1}\varepsilon, \quad \kappa_a = \kappa_{a0} + \kappa_{a1}\varepsilon, \quad 0 \leq \varepsilon \leq \varepsilon_*$$

$$\Gamma_a = \Gamma_a^\circ, \quad \kappa_a = \kappa_a^\circ, \quad \varepsilon_* < \varepsilon < \infty. \tag{43}$$

The parameter Γ_a° equals the maximal attempt rate for separation of active strands in a mechanically activated medium, whereas the constant κ_a° stands for the maximal concentration of active MRs.

The sum of the mass fraction of crystallites, $\kappa_c = 0.37$, and the maximal concentration of active MRs, $\kappa_a^\circ = 0.38$, is less than unity, which implies that the mass fraction of the passive amorphous phase (where reformation of strands does not occur) in the vicinity of the apparent yield point is estimated as $\kappa_p = 0.25$.

CONCLUSIONS

Constitutive equations were derived for the time-dependent behavior of semicrystalline polymers at isothermal loading with small strains. To develop stress–strain relations, a version of the mean-field approach is employed: a complicated microstructure of a semicrystalline polymer is replaced by an equivalent transient network of macromolecules bridged by junctions (physical crosslinks, entanglements, and crystalline lamellae). The network is assumed to be strongly heterogeneous, and it is thought of as an ensemble of mesoregions with various activation energies for separation of strands from temporary nodes.

With reference to the theory of transient networks, the viscoelastic response of a polymer is ascribed to the processes of separation of active strands from temporary junctions and attachment of dangling chains to the network in active mesodomains. Rearrangement of active strands is modeled as a thermomechanically activated process whose rate is determined by the Eyring formula.

The viscoplastic response is described by sliding of junctions with respect to their reference positions in the bulk material. In a virgin specimen, only part of the junctions is mobile, whereas the other part is immobilized by surrounding lamellae. Straining of a specimen causes fine and coarse slip of lamellar blocks, which, in turn, induce activation of extra junctions. This process proceeds until all junctions become mobile. The rate of sliding of junctions is assumed to be proportional to the macrostress in a specimen.

The mechanical energy of a semicrystalline polymer is determined as the sum of the strain energies of strands in active and passive mesodomains. Constitutive equations are derived by using the laws of thermodynamics. These relations are applied to study stretching of a specimen with a constant strain rate and relaxation of longitudinal stresses at several strains in the vicinity of the apparent yield point.

A series of relaxation tests were performed on isotactic polypropylene at room temperature. Adjustable parameters in the stress–strain equations are found by fitting observations. The following conclusions are drawn from the analysis of experimental data:

1. The average potential energy for separation of strands from temporary junctions in active MRs Ω and the standard deviation of potential energies Σ are not affected by mechanical factors.
2. The concentration of active MRs κ_a increases with strain ε and reaches its threshold value κ_a° at some strain ε_*, in the close vicinity of the apparent yield strain ε_y.
3. The attempt rate for detachment of active strands from temporary nodes Γ_a grows with strain ε and reaches its maximum value at the same strain ε_*.

4. The initial concentration of mobile junctions $\eta(0)$ is negligibly small (about 4%), but it rapidly increases with strain. Mechanically induced activation of all junctions occurs at the strain ε_0, which is rather close to the apparent yield strain ε_y. This implies that the apparent yield point may be associated with the strain at which all junctions in a network begin to slide with respect to their reference positions in the bulk medium.

References

1. Roetling, J. A. Polymer 1965, 6, 311.
2. Roetling, J. A. Polymer 1965, 6, 615.
3. Roetling, J. A. Polymer 1966, 7, 303.
4. Peterlin, A.; Balta-Calleja, F. J. J Appl Phys 1969, 40, 4238.
5. Peterlin, A. J Mater Sci 1971, 6, 490.
6. Meinel, G.; Peterlin, A. J Polym Sci Polym Phys Ed 1971, 9, 1967.
7. Flory, P. J.; Yoon, D. Y. Nature 1978, 272, 226.
8. Gent, A. N.; Madan, S. J. J Polym Sci Polym Phys Ed 1989, 27, 1529.
9. Seguela, R.; Staniek, E.; Escaig, B.; Fillon, B. J Appl Polym Sci 1999, 71, 1873.
10. Ward, I. M.; Hadley, D. W. An Introduction to the Mechanical Properties of Solid Polymers; Wiley: New York, 1993.
11. Eyring, H. J Chem Phys 1936, 4, 283.
12. Argon, A. S. J Macromol Sci Phys 1973, B8, 573.
13. Bowden, P. B.; Raha, S. Phil Mag 1974, 29, 149.
14. Bordonaro, C. M.; Krempl, E. Polym Eng Sci 1992, 32, 1066.
15. Bordonaro, C. M.; Krempl, E. Polym Eng Sci 1995, 35, 310.
16. Bowden, P. B.; Young, R. J. J Mater Sci 1974, 9, 2034.
17. Young, R. J. Phil Mag 1974, 30, 85.
18. Crist, B.; Fisher, C. J.; Howard, P. R. Macromolecules 1989, 22, 1709.
19. O'Kane, W. J.; Young, R. J.; Ryan, A. J. J Macromol Sci Phys 1995, B34, 427.
20. Kennedy, M. A.; Peacock, A. J.; Failla, M. D.; Lucas, J. C.; Mandelkern, L. Macromolecules 1995, 28, 1407.
21. Coulon, G.; Castelein, G.; G'Sell, C. Polymer 1998, 40, 95.
22. Brooks, N. W.; Ghazali, M.; Duckett, R. A.; Unwin, A. P.; Ward, I. M. Polymer 1999, 40, 821.
23. Brooks, N. W. J.; Mukhtar, M. Polymer 2000, 41, 1475.
24. Sirotkin, R. O.; Brooks, N. W. Polymer 2001, 42, 3791.
25. Takayanagi, M.; Imada, K.; Kajiyama, T. Polym Symp 1965, 15, 263.
26. Keith, H. D.; Padden, F. J.; Vadimsky, R. G. J Polym Sci A-2 1966, 4, 267.
27. Takayanagi, M.; Nitta, K. Macromol Theory Simul 1997, 6, 181.
28. Nitta, K.-H.; Takayanagi, M. J Polym Sci Part B: Polym Phys 1999, 37, 357.
29. Nitta, K.-H.; Takayanagi, M. J Polym Sci Part B: Polym Phys 2000, 38, 1037.
30. Ward, I. M.; Wolfe, J. M. J Mech Phys Solids 1966, 14, 131.
31. Smart, J.; Williams, J. G. J Mech Phys Solids 1972, 20, 313.
32. Ariyama, T. Polym Eng Sci 1993, 33, 18.
33. Ariyama, T. Polym Eng Sci 1993, 33, 1494.
34. Ariyama, T. J Mater Sci 1996, 31, 4127.
35. Ariyama, T.; Mori, Y.; Kaneko, K. Polym Eng Sci 1997, 37, 81.
36. Wortmann, F.-J.; Schulz, K. V. Polymer 1994, 35, 2108.
37. Wortmann, F.-J.; Schulz, K. V. Polymer 1995, 36, 2363.
38. Dutta, N. K.; Edward, G. H. J Appl Polym Sci 1997, 66, 1101.
39. Read, B. E.; Tomlins, P. E. Polymer 1997, 38, 4617.
40. Tomlins, P. E.; Read, B. E. Polymer 1998, 39, 355.
41. Fricova, O.; Olcak, D.; Sevcovic, L.; Durcova, O. Acta Polym 1998, 49, 495.
42. Andreassen, E. Polymer 1999, 40, 3909.
43. Lopez-Manchado, M. A.; Arroyo, M. Polymer 2000, 41, 7761.
44. Gallego Ferrer, G.; Salmeron Sanchez, M.; Verdu Sanchez, E.; Romero Colomer, F.; Gomez Ribelles, J. L. Polym Int 2000, 49, 853.
45. Souza, A. M. C.; Demarquette, N. R. Polymer 2002, 43, 1313.
46. Verma, R.; Marand, H.; Hsiao, B. Macromolecules 1996, 29, 7767.
47. Zhang, X. C.; Butler, M. F.; Cameron, R. E. Polym Int 1999, 48, 1173.
48. Bergstrom, J. S.; Kurtz, S. M.; Rimnac, C. M.; Edidin, A. A. Biomaterials 2002, 23, 2329.
49. Meyer, R. W.; Pruitt, L. A. Polymer 2001, 42, 5293.
50. Sweeney, J.; Ward, I. M. J Rheol 1995, 39, 861.
51. Sweeney, J.; Ward, I. M. J Mech Phys Solids 1996, 44, 1033.
52. Llana, P. G.; Boyce, M. C. Polymer 1999, 40, 6729.
53. Boyce, M. C.; Socrate, S.; Llana, P. G. Polymer 2000, 41, 2183.
54. Green, M. S.; Tobolsky, A. V. J Chem Phys 1946, 14, 80.
55. Yamamoto, M. J Phys Soc Jpn 1956, 11, 413.
56. Lodge, A. S. Rheol Acta 1968, 7, 379.
57. Tanaka, F.; Edwards, S. F. Macromolecules 1992, 25, 1516.
58. G'Sell, C.; Jones, J. J. J Mater Sci 1979, 14, 583.
59. Duffo, P.; Monasse, B.; Haudin, J. M.; G'Sell, C.; Dahoun, A. J Mater Sci 1995, 30, 701.
60. Duan, Y.; Saigal, A.; Grief, R.; Zimmerman, M. A. Polym Eng Sci 2001, 41, 1322.
61. Derrida, B. Phys Rev Lett 1980, 45, 79.
62. Collar, E. P.; Cofrades, A. G.; Laguna, O.; Areso, S.; Garcia-Martinez, J. M. Eur Polym J 2000, 36, 2265.
63. Wunderlich, B. Crystal Melting; Macromolecular Physics, Vol. 3; Academic Press: New York, 1980.